

AN ULTRA-VIOLET LIGHT MONITOR FOR SPEAR3

C.Limborg*, A.Ringwall, M.Rowen, J.Stieber

Stanford Linear Accelerator Ctr, Stanford Univ., Stanford, CA 94309, USA

Abstract

A synchrotron light monitor is an essential tool for operating a storage ring. For SPEAR3, the upgrade of the SPEAR storage ring, the light monitor was designed not only for monitoring the beam presence but also to measure beam parameters. To minimize diffraction effects, UV light around 200 nm is used to image the electron source rather than visible light. At 200 nm, the rms diffraction spot is 14 μm , much smaller than the rms beam sizes 180 μm horizontally and 51 μm vertically. A mask will absorb the x-ray fan of synchrotron radiation. The outer core of the light cone is reflected by a 9 degrees grazing incidence flat silicon mirror coated with rhodium. A telescopic system, of the Cassegrain type, with 2 on-axis spherical mirrors, images the source. The magnification can be varied from 1:1 to 8:1 but the system is optimized for a 3:1 magnification. Reflective optics was chosen to maximize the flux by permitting large bandwidth in a chromatic aberration-free system. Tolerances on the optics needed for high quality imaging are discussed.

1 SOURCE AND BEAMLINE

1.1 Introduction

The optical diagnostics beamline presented in this paper is being built on SPEAR3, the new low emittance, 18 mrad, high current, 500 mA, storage ring to replace the existing one at SSRL. SPEAR3 will be commissioned in early 2004. We discuss the principal components of the beamline, the characteristics of the extraction mirrors and of the reflective optics system used to image the electron beam with UV synchrotron light.

1.2 Source

SPEAR3 will operate at 3 GeV and the source for the diagnostic beam line will be near the end of one of the combined function bend magnets. At the source, the magnetic field is 1.274 T ($\rho = 7.852\text{m}$, $E_c = 7.5$ keV) and the electron beam sizes are respectively in the horizontal and vertical planes $\sigma_x = 182$ μm and $\sigma_y = 51$ μm for a 1% coupling.

Masks will limit the horizontal acceptance to ± 1.75 mrad and the vertical acceptance to ± 3 mrad. The source longitudinal extension is then 27.5 mm. The apparent horizontal extension from the single electron trajectory (sagitta) is 12 μm . The apparent vertical source extension is 41.5 μm for a single electron. This is large with respect to the diffraction spot of 14 μm . Two sets of slits, one vertical and one horizontal will be used to reduce the

apparent vertical beam size. The horizontal opening angle of ± 1.75 mrad was kept to leave the flexibility of studying near IR radiation, however the source extension will be reduced to ± 10 mm for the nominal tuning (see depth of field 2.4).

1.3 Transport Line

- Cold finger

A water-cooled copper bar, referred to as a cold finger, absorbs the central ± 0.45 mrad of the bending magnet radiation. The cold finger, located at 8.5 m from the source, will absorb 99.1% of the total power in the case of nominally steered beam while passing most of the long wavelength and therefore out of plane radiation. Figure 1 shows the flux as a function of vertical opening angle. The cold finger shadows the area between the vertical lines suppressing only a small fraction of the total flux.

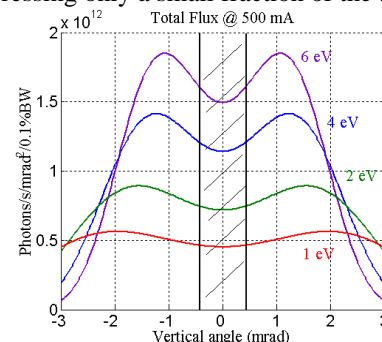


Figure 1. Spectral flux vs vertical opening angle computed for 500 mA.

- Permanent magnet deflector

A permanent magnet at the front end of the beam line will deflect any electrons from the storage ring into a stop, allowing the synchrotron light monitor line to be open safely in all operating modes.

- Extraction mirror

The first mirror is used as a low pass filter, prior to any view ports between the laboratory and the SPEAR3 vacuum system. It horizontally deflects the light at a 9 degrees grazing incidence into the area available for the optical station. Among the various coating materials available, rhodium was chosen as its reflectivities for 200 nm (6 eV) at 9 degrees grazing incidence are respectively 0.92 and 0.62 for the σ - and π - polarizations. Rhodium also has high performance in the visible and IR regions. It has a good UHV compatibility and does not damage with radiation. This silicon based mirror must be able to tolerate the full power of a mis-steered beam, with 72.65 W per horizontal mrad. At 9.63 m from the source this mirror can take the full power load of the mis-steered beam with a simple clamped cooling bar through an indium interface material. The mirror is positioned

kinematically giving the 6 degrees of freedom for alignment. The pitch about the vertical axis will be remote controlled to 7 μrad step sizes.

An excimer grade quartz window, 0.25 inch thick, will provide the seal to the vacuum. It will be positioned the furthest to minimize darkening due to x-ray scattering.

- Radiation box

The Fluka Monte-Carlo code predicts a maximum of 70 mrem/hour dose in the optical laboratory produced from secondary X-ray emission from mis-steered beam striking the primary mirror. This dose level will be reduced to less than 0.7mrem/hour by reflecting the light exiting the tunnel off two mirrors, M1 and M2, at 6.25 degrees from normal incidence, contained in a lead shielded box. Those mirrors are coated with oxide free aluminum which has a reflectivity of 0.92 between 2eV and 6 eV.

2 CASSEGRAIN SYSTEM

2.1 Description

To suppress chromatic aberrations and thus offer the possibility of using large bandwidths, a reflective optics imaging system was designed using the Zemax code [3]. The system consists of a concave spherical mirror M3 ($\rho = 3860.83$ mm radius of curvature) and a convex spherical mirror M4 ($\rho = 327.57$ mm) separated by 2 m. Those mirrors are used on axis, at normal incidence. M3 has a 10 mm diameter hole to let the light bouncing back from M4 pass through its center. This geometry corresponds to a Cassegrain system. A detailed analytic description of the system has been given in [1,2]. The good quality optical area of the M3 mirror will have outer and inner optical diameters of 112 mm and 16 mm respectively. The M4 mirror has an outside diameter of 13 mm with a good optical area of 8.4 mm diameter. The M4 mount and positioner will be confined to the cold finger shadow, 14.7 mm high. Similarly the shadow of the cold finger at the M3 mirror is 16.5 mm high, larger than the inner diameter of the good optical area.

2.2 Flexibility

The system parameters given above were optimized for a magnification of 3:1, with the image plane 4 m downstream of M4. However, keeping the position of M3 and the two mirror dimensions fixed, but changing the relative position of M4 from M3, any magnification between 8:1 and 1:1 can be obtained. Table 2 summarizes parameters for those various tunings.

Magnification	1:1	3:1	5:1	8:1
d (mm)	2012.8	2000	1997.4	1996.0
f (mm)	1227.6	4000	6758.5	10870
rms spot size(μm)	1.4	4.1	6.8	10.8

Table2: Magnifications obtained when displacing M4 from M3 ($M3M4 = d$); the focal distance, f, is given from M4. The rms spot size is computed from a point source. The total excursion on M4 ranges between +13 mm, -5 mm from the position for the 3:1 magnification case. The same range of magnification can be achieved by keeping

M4 fixed and moving M3, but this would require a displacement range between -300mm to +900mm for M3.

2.3 Spherical aberrations

The rms spot size referred to below corresponds to the rms image size of a single source point. Figure 2.1 shows the evolution of rms spot size at focus when varying the opening angle. Figure 2.2 shows the change in optimum focus location as a function of opening angle. Horizontal and vertical slits will be used to adjust the opening angles to have the optimum focus in both planes at the same time.

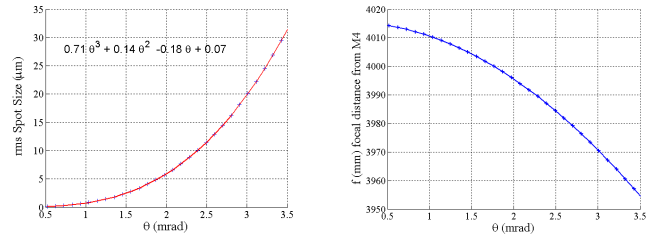


Figure 2.1: rms spot size vs opening angle

Figure 2.2: focal distance from M4 vs opening angle

Both curves are computed for a 3:1 magnification

2.4 Depth of field

With a ± 1.75 mrad horizontal opening angle, the longitudinal source extension available is 27.5 mm long. This was chosen to leave the possibility to measure low energy photons. However, the depth of field needs to be reduced to ± 10 mm around the central source point to have rms spot size of the extreme points of the source closer to the diffraction spot size, as indicated in table3.

x(mm)	-15	-10	-5	0	+5	+10	+15
rms(μm)	54.5	35.6	16.7	4.1	21.7	40.5	59

Table 3: rms spot size vs source point displacement x from central source point for the 3:1 configuration and a ± 1.75 mrad opening angle. Those numbers are to be compared to 45 μm which is the 3 times magnified rms image of the diffraction spot size.

2.5 Tolerance on radius of curvature

Manufacturing errors on the spherical mirrors radii can be compensated by adjusting the distance d from M3 to M4. Table 4 shows that the position of M4 will not vary by more than 25 mm from nominal if the radius of curvature deviates by less than $\pm 1\%$ from the specifications. The focal distance, f, from M4 will then also be modified from the ideal case. With the corrected values in d and f, the rms spot size remains 4 μm .

nominal	Δ	Case + d / f	Case - d / f
$\rho_3 = 3860.82$	$\pm 1\%$	2024 / 3954	1975.8 / 4046.6
$\rho_4 = 327.57$	$\pm 4\%$	1993.7 / 4160	2006.3 / 3839.1

Table 4. d : variation of distance between M3 –M4; f : distance to focus from M4 for errors on radii of curvature

3 SURFACE QUALITY OF MIRRORS

The tolerances on slope error and roughness for the five mirrors of the system are defined such that the rms spot size (extension from a single source point image) stays smaller than the rms of the ideal electron beam image. The ideal image of the source is the convolution of the electron beam size by the single electron diffraction image (14 μm rms for 200nm wavelength). The electron beam rms sizes are 182 μm horizontally and 51 μm vertically for 1% coupling. Since all but the M0 mirror are operated at or near normal incidence the surface quality specification will be that required for maintaining a good vertical image. The M0 mirror will have different specifications in the tangential and sagittal directions.

3.1 Modeling figure errors

Slope errors for the 5 mirrors of the system were modeled by introducing a modulation of amplitude on the surface of the mirrors. This modulation is represented by a function $f = A [1 - \cos(2\pi W x)]$ where A is the amplitude of the modulation, W is the wave number and x can be either the horizontal, vertical or radial dimension. The slope error function is then given by $f' = 2\pi W A \sin(2\pi W x)$. The PTV slope error is given by $4\pi W A$ rad and the rms slope error is given by $\sqrt{2}\pi W A$ rad. For all wavelengths smaller than the dimension along which we study the effect of the modulation, the slope error does not depend on the wavelength. The roughness value, equivalent to the amplitude A , depends on the wavelength. Roughness values are given for wavelengths smaller than 1 mm and slope errors for wavelengths larger than 1mm.

3.2 Single mirror tolerances

- Extraction mirror: M0

Rms slope errors of 7.8 μrad horizontally and 4.9 μrad vertically are needed to keep the single point rms image sizes respectively below 150 μm and 15 μm , respectively in the horizontal and vertical planes.

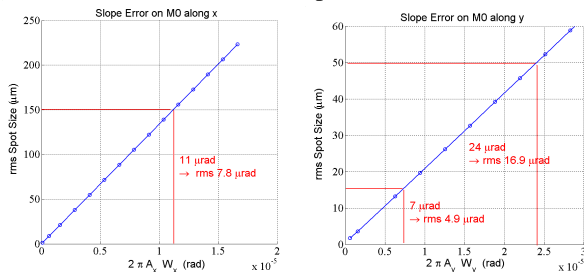


Figure 3: rms spot size as a function of slope error amplitudes for wavelengths larger than 1 mm; magnification of 1:1

- Flat mirrors : M1 and M2

Rms slope errors of 0.53 and 0.5 μrad are needed to keep the single point rms image sizes smaller than 15 μm , respectively for the two flat mirrors M1 and M2.

- Spherical mirrors: M3 and M4

For M3/M4, rms slope errors of 0.42/6.22 μrad are needed to keep the single point rms image sizes below 15 μm .

Slope error tolerances as low as 0.5 μrad can be met for the four mirrors M1, M2, M3 and M4 according to optical manufacturers [5]. For the five mirrors, a 10 rms roughness at frequencies less than 100 μm would result in some undesirable degradation of the image quality.

3.3 Combination of errors

The rms spot size was computed when combining slope errors on the five mirror at the same time. Slope errors of 1 μrad , 0 μrad and -1 μrad rms in the vertical plane were used for each mirror. That gives 243 possible combinations for the set of the 5 mirrors. When the slope error is zero, the mirror is considered to be perfect. Figure 4 shows that 70% of the 243 cases give rms spot sizes below 51 μm .

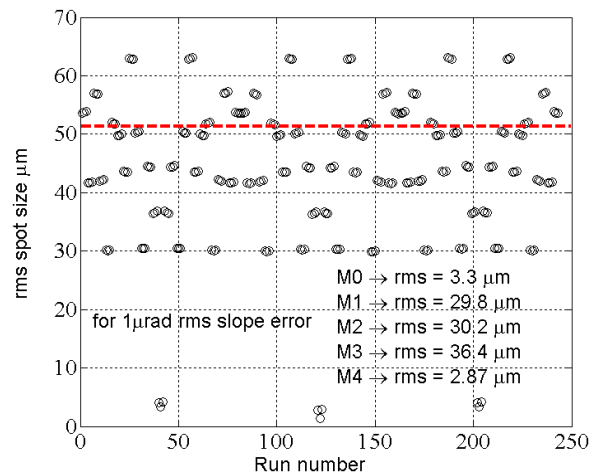


Figure 4: rms spot size vs run number for combinations of rms slope errors of -1, 0, 1 μrad on the 5 mirrors; magnification of 1:1

ACKNOWLEDGEMENTS

The authors would like to thank J.Liu for the Fluka studies. They are grateful to T.Rabedeau, P.Stefan, J.Sebek, J.Corbett, N.Kurita, R.Hettel, M.Cornacchia, T.Elioff and A.Fisher for valuable discussions. This work was supported by the Department of Energy under contract DE-AC03-76SF00515.

REFERENCES

- [1] S.Rosin , "Inverse Cassegrainian Systems", Aug 1968, Vol.7 No.8 Applied Optics 1483
- [2] Born & Wolf , "Principles of Optics", p 246
- [3] C.Limborg et al. "SPEAR 3 Technical Note", SPEAR 3 Technical Note.
- [4] Zemax code "ZEMAX-EE Optical Design Program", Focus Software
- [5] SESO, Societe Europeene de Systemes Optiques "Private communications with JJ.Ferme"